

Fig. 5. Cavity gas-pressure instrumentation gage signal from alcove 4: 100-kpsi-range Norwood gage, 2 msec/cm, 25 kpsi/cm.

Figure 6 shows only the initial pulses. Further details of these stress-gage measurements are given in Table 2 in section 3, where a comparison with the calculations is made.

Postshot Measurements

Chemical tracer distribution. Five chemical tracer sections were fabricated and mounted at different locations along the tunnel to determine the quantity of wall material ablated by the passage of the shock wave and flow behind the shock. Each section was a 1-meter i.d., 6.1-meter long laminated right circular cylinder composed of two separate concentric layers containing different tracers. The thickness and quantity of tracers in each layer varied with location along the tunnel. The tracers were commercial-grade chemicals mixed with cement to form a loaded grout or concrete. Figure 7 and Table 1 show the locations of each section,

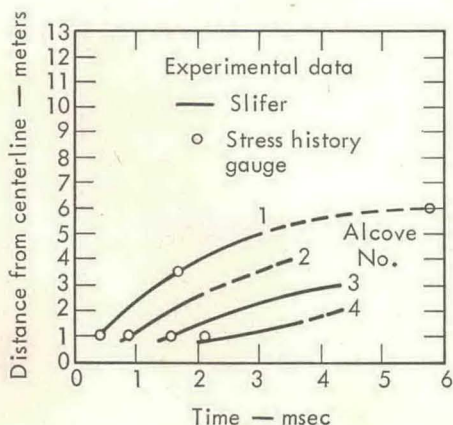


Fig. 6. Slifer and stress gage TOA data for shock-front position in the alcoves.

thickness of the layers, and different tracers used. The inner layer for each section was the tunnel wall. Consequently, ablation of the inner layer had to occur before ablation of the outer layer could begin.

Mass spectrometer analyses of the postshot drill samples are shown in Figure 7 for the first three sections (L. A. Rogers, private communication, 1968). Tracers from these sections were distributed all along the tunnel, with the highest concentration at the 90- to 100-meter position. This position corresponds to the stagnation location of the flow discussed later. Results for the last two sections (not shown) indicated that only a small quantity of the inner layer was ablated.

Cavity formation and the subsidence crater. Chemical analyses of refractories from post-shot drill cores suggested a significant non-spherical shape for the final cavity geometry just prior to collapse. The extent and relative

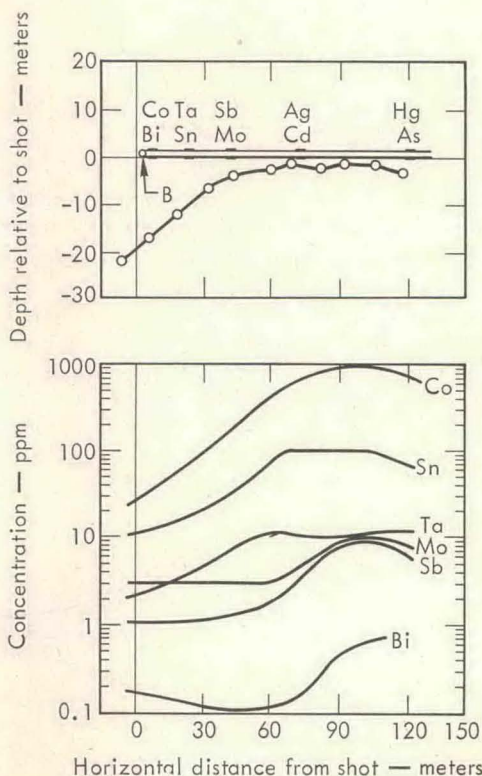


Fig. 7. The chemical tracers and their distribution. Upper figure: Location of chemical tracers in the tunnel and location of postshot samples. Lower figure: Analysis of the final tracer distribution.

TABLE 1. Chemical Tracers and Ablation Results

Layer	Tracer	Distance to Center of Tracer Section, meters	Thickness, cm	Inferred Minimum Ablation Thickness, † cm	Estimated Wall Mass Ablated, kg/m
A*	Co	6.1	10.2	>10.5	>134
B	Bi		0.3		
A*	Ta	21.4	5.1	>5.1	>4.4
B	Sn		2.5		
A*	Sb	39.6	2.5	>2.5	>1.6
B	Mo		1.3		
A*	Ag	70.2	1.3	<1.3	<0.9
B	Cd		1.3		
A*	Hg	119.0	0.3	<0.3	<1.0
B	As		5.1		

* Adjacent to the tunnel air.

† Inferred from Figure 7.

dimensions of the cavity at that time are illustrated in Figure 8 (L. A. Rogers, private communication, 1968). Further evidence of the nonspherical cavity growth is given by the asymmetric subsidence crater shown in Figure 9. The shot point was directly below the north edge of the concrete access-shaft pad, and the tunnel ran west, parallel to the cable tray. Thus the collapse crater extended at the surface from a few meters east of the shot point to approximately 60 meters along the tunnel.

3. NUMERICAL SIMULATION

Numerical Codes

To consider simultaneously the time histories of the two shocks, down the tunnel and into the surrounding alluvium, the Tensor-Puff [Crowley and Barr, 1971] code was developed. Tensor-Puff is the combination of two finite-difference codes, Tensor [Maenchen and Sack, 1964] and Puff [Crowley, 1967]. These codes, which increment the partial differential con-

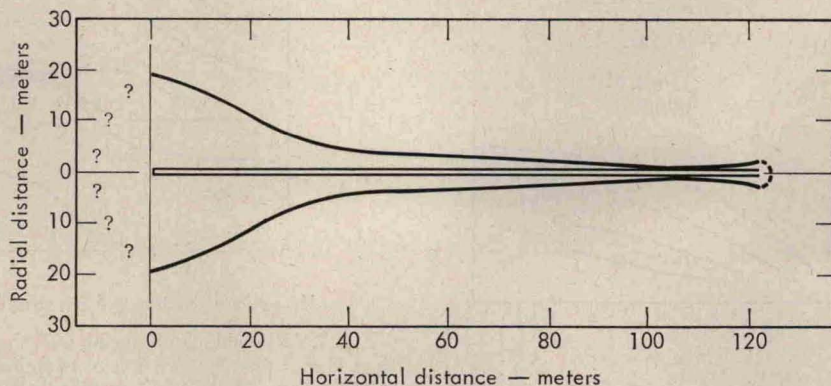


Fig. 8. Shape of the cavity before collapse, inferred from the postshot drilling data.